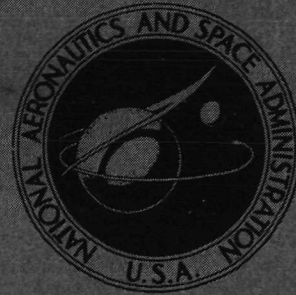


N72-14935

**NASA TECHNICAL
MEMORANDUM**



NASA TM X-2447

NASA TM X-2447

**CASE FILE
COPY**

**COMPARISON OF THE RADIATION FLUX
PROFILES AND SPECTRAL DETAIL FROM
THREE DETAILED NONGRAY RADIATION
MODELS AT CONDITIONS REPRESENTATIVE
OF HYPERVELOCITY EARTH ENTRY**

by John T. Suttles

Langley Research Center

Hampton, Va. 23365

1. Report No. NASA TM X-2447	2. Government Accession No.	3. Recipient's Catalog No.	
4. Title and Subtitle COMPARISON OF THE RADIATION FLUX PROFILES AND SPECTRAL DETAIL FROM THREE DETAILED NONGRAY RADIATION MODELS AT CONDITIONS REPRESENTATIVE OF HYPERVELOCITY EARTH ENTRY		5. Report Date January 1972	6. Performing Organization Code
		8. Performing Organization Report No. L-7986	10. Work Unit No. 117-07-04-08
7. Author(s) John T. Suttles		11. Contract or Grant No.	
9. Performing Organization Name and Address NASA Langley Research Center Hampton, Va. 23365		13. Type of Report and Period Covered Technical Memorandum	
		14. Sponsoring Agency Code	
12. Sponsoring Agency Name and Address National Aeronautics and Space Administration Washington, D.C. 20546		15. Supplementary Notes	
16. Abstract <p>Three detailed nongray radiation models have been compared on the basis of the approaches used for the transport calculations and absorption coefficients and of results obtained for the radiation flux profiles and spectral distributions. The calculated results were for shock-layer conditions representative of manned earth reentry from an interplanetary mission. The three models are RATRAP developed by Wilson (LMSC 6-77-67-12), RADICAL developed by Nicolet (NASA CR-1656), and MDAC developed by Rigdon, Dirling, and Thomas (NASA CR-1462). The results have shown that significant differences exist in the radiation flux computed by the three models. The RADICAL model was found to depend on fewer approximations, to include more detail, and to require less computer time than the other models.</p>			
17. Key Words (Suggested by Author(s)) Radiative heat flux Aerodynamic heat transfer		18. Distribution Statement Unclassified - Unlimited	
19. Security Classif. (of this report) Unclassified	20. Security Classif. (of this page) Unclassified	21. No. of Pages 27	22. Price* \$3.00

COMPARISON OF THE RADIATION FLUX PROFILES AND
SPECTRAL DETAIL FROM THREE DETAILED NONGRAY RADIATION
MODELS AT CONDITIONS REPRESENTATIVE OF
HYPERVELOCITY EARTH ENTRY

By John T. Suttles
Langley Research Center

SUMMARY

Three detailed nongray radiation models have been compared on the basis of the approaches used for the transport calculations and absorption coefficients and of results obtained for the radiation flux profiles and spectral distributions. The calculated results were for shock-layer conditions representative of manned earth reentry from an interplanetary mission. The three models are RATRAP developed by Wilson (LMSC 6-77-67-12), RADICAL developed by Nicolet (NASA CR-1656), and MDAC developed by Rigdon, Dirling, and Thomas (NASA CR-1462). The results have shown that significant differences exist in the radiation flux computed by the three models. The RADICAL model was found to depend on fewer approximations, to include more detail, and to require less computer time than the other models.

INTRODUCTION

In recent years the problem of hypervelocity entry into the earth's atmosphere has received much attention in the literature (for example, see refs. 1 to 3). When results of the various calculations are compared, it is found that considerable differences exist in the radiative heating rates predicted. The question then arises as to whether the differences are due to the flow-field calculation methods or the radiation models used. The resolution of this question is a prerequisite to a meaningful evaluation of the work which has been done.

In the past few years a set of computer programs has been developed at the Langley Research Center to calculate the flow field and radiation flux for both ablating and non-ablating bodies (ref. 1). For the computational technique described in reference 1, a detailed nongray radiation computer code called RATRAP (ref. 4) was used to calculate the radiation heat flux which is coupled to the flow computations. During the course of using the method two other detailed nongray radiation computer codes became available.

These are the RADICAL code (ref. 5) and the MDAC code (ref. 3). Subsequently, flow-field results obtained by the method of reference 1 were used as a common set of conditions for calculating radiative heat fluxes with the available radiation codes. From these calculations results from the three radiation codes, RATRAP, RADICAL, and MDAC, could be compared for flow-field conditions of interest. The purpose of this paper is to present the results of such a comparison.

SYMBOLS

$\check{C}_N, \check{C}_O, \check{C}_C, \check{C}_H$ mass fraction of the elements nitrogen, oxygen, carbon, and hydrogen, respectively

$h\nu$ photon energy, eV

L/D lift-drag ratio

\dot{m} heat-shield mass-flux rate, g/cm^2 -sec

p pressure, atm (1 atm = 101 325 N/m²)

q_R radiative flux, W/cm²

R_N spherical nose radius, cm

T temperature, K

V velocity, km/sec

$\frac{W}{C_D A}$ ballistic coefficient, N/m²

y distance from body along the normal to body, cm

γ reentry angle (measured below local horizontal), deg

δ shock standoff distance, cm

ϵ dummy variable of integration

ρ density, g/cm³

Subscripts:

C	continuum radiation contribution
E	earth relative value at 121.92 km
L	atomic-line radiation contribution
shock	postshock value
∞	free-stream value

METHOD

Flow-Field Properties

The comparisons for the present paper were made by selecting a typical set of trajectory conditions and using the method of reference 1, which includes the RATRAP radiation code, to compute a flow-field solution. This flow-field solution was used for all the radiation calculations. The conditions chosen were based on the values for the peak heating point on the trajectory given in figure 1. This figure shows the altitude-velocity plot of a typical lifting-entry trajectory for interplanetary return speeds of a manned spacecraft. A spherical body with a radius of 342.7 cm was selected and a phenolic-nylon material was used for the heat shield. The flow-field calculations produced the stagnation-streamline temperature profile shown in figure 2. Three important regions comprise the shock layer: the inviscid-air region, where the temperature decreases from about 14 000 K to 10 000 K as a result of nonadiabatic effects; the mixing region, where the temperature decreases from about 10 000 K to about 3300 K as a result of viscous effects; and the ablation-gas region, which is nearly isothermal at about 3300 K. For the conditions shown the postshock pressure is 0.41 atmosphere and the total shock-layer thickness is 16.94 cm.

Also of interest for the radiation computations are the species mole fractions in the shock layer which are shown in figure 3. These results illustrate that the inviscid-air region is a plasma composed of electrons and atomic and ionic nitrogen and oxygen. In the ablation-gas region next to the wall the species present are primarily H_2 , H, CO , and various hydrocarbons with a small amount of CN and some trace species not shown. The mixing region is composed of a mixture of the species found in the two adjacent regions along with some atomic carbon. Note that the mass fractions of the elements which comprise the phenolic-nylon heat shield are shown in the figure. The heat-shield mass-flux rate obtained for this case is $0.0578 \text{ g/cm}^2\text{-sec}$ ($\dot{m}/\rho_\infty V_\infty = 0.19$). The flow-field results

shown in figures 2 and 3 were used to compute radiative heating toward the body with the three detailed, nongray radiation computer codes, RATRAP, RADICAL, and MDAC.

Radiation Models

Features of the radiation models used are compared in tables I and II. The methods used in the transport calculations are given in table I, and the approaches used in the absorption-coefficient models are presented in table II. The comparison of absorption-coefficient models has been divided into continuum contributions, which include molecular bands, and atomic-line contributions.

For the transport calculations the major point of interest is the approaches to solving the transport equation. In RATRAP and RADICAL the equation is reduced analytically to a quadrature expression for the heat flux and the "exponential approximation" is used. The form of the approximation assumed in both codes is

$$E_3(x) \approx \frac{1}{2} e^{-2x}$$

where E_3 is the exponential integral of order 3. The effect of using this approximation is discussed in reference 6 where it is indicated that results within about 10 percent of exact calculations are obtained for the condition of unit optical depth. The approximation is exact in the optically thin and thick limits. In contrast, MDAC integrates the transport equation numerically for the intensity along eight slant rays in the plane slab. The flux is obtained by integrating the intensity over solid angle with a Gaussian quadrature formula.

From a comparison of the methods of treating the continuum absorption coefficients (table II(a)), it is seen that the RATRAP and RADICAL codes utilize the works of Biberman and Norman (ref. 7) and Wilson and Nicolet (ref. 8), whereas MDAC utilizes the hydrogenic models of references 9 and 10. The methods used in references 7 and 8 are more realistic descriptions of the complex atom processes than the hydrogenic approaches of references 9 and 10. For the molecular bands, each of the codes uses the same type of description (refs. 3, 5, 11, and 12).

The approaches for the line absorption coefficients (table II(b)) are diverse. A comparison indicates that the RADICAL code includes an individual treatment of the lines, more of the line shape and broadening mechanisms, and more spectral detail and uses realistic line strengths in all cases. In general, it is concluded that as far as the line models, RADICAL involves fewer approximations and includes more detail than the other codes.

The various radiating species that are included in each of the codes are shown in table III for atomic (and ionic) species and in table IV and figure 4 for molecular species. Absorption-coefficient data such as oscillator strengths and absorption cross sections

are described in references 6 and 11 for the RATRAP code and in references 5 and 3 for RADICAL and MDAC, respectively. It should be pointed out that a more recent version of the RATRAP code is available which does include carbon and hydrogen atomic lines; however, that version was not used in this work. Calculations with the later version have shown that the results presented in this study are not affected by differences in the two versions of the code.

In figure 4 it is important to note the windows between 6 and 7 eV and between 10 and 11 eV in the spectral range of the molecular contributions in RATRAP. The RADICAL and MDAC codes include several molecular contributions in these spectral ranges. As will be shown later, the existence of the hydrogen molecular (H_2) contribution in the range 10 to 11 eV has an important influence on the heating which reaches the body surface. The window between 6 and 7 eV is found to be of less importance, but nevertheless it influences the spectral distribution of the heat flux which reaches the body.

In references 6 and 5 comparisons with available data and other predictions are made for RATRAP and RADICAL, respectively. To the author's knowledge such an evaluation of the MDAC code has not been made.

RESULTS AND DISCUSSION

Gray-Gas Heat Fluxes

Before the calculations for shock-layer heat fluxes are shown, heat fluxes for a gas with a gray absorption coefficient (0.05 cm^{-1}) and temperature varying linearly from 8000 K at the body surface to 14 000 K at the shock wave are compared. This comparison allows the methods used in the transport calculations to be evaluated independently of the absorption-coefficient models. Results for heat flux toward the body are shown in figure 5. Calculations are presented from RATRAP both with and without the exponential approximation to demonstrate that this approximation causes the deviation of the results for RATRAP and RADICAL from those of MDAC. The maximum deviation is about 14 percent and occurs near the peak of the flux profile. Since the results for RATRAP and RADICAL agree when the exponential approximation is used, calculations for RADICAL without the approximation have not been shown.

The calculations presented in the remainder of this study were obtained with the exponential approximation in the RATRAP and RADICAL codes. Thus in comparing results from these codes with those of MDAC, some deviations will be caused by the approximation. However, since the approximation is exact in the optically thick limit, and since the nongray case to be presented is optically thicker than the gray case shown, the deviations are expected to be less than those shown in figure 5. As will be discussed

later, a calculation of the continuum flux using RATRAP without the exponential approximation has shown the deviation to be less in the nongray case.

Shock-Layer Heat Fluxes

The shock-layer properties and radiation models described previously have been used to calculate the spectral radiation heat flux. The calculations are for the stagnation streamline and only the radiation heat flux toward the body is considered. To facilitate the comparisons, the results have been separated into "line flux" and "continuum flux." In the RATRAP and RADICAL codes the separation of the results into continuum-only and line (difference between continuum-only and total) contributions was included as part of the formulation of the model. For the MDAC results the total flux was calculated. The input data for line transition were then removed and a calculation with only continuum transitions was made. The line contribution was obtained by subtracting the continuum from the total. Thus each of the codes has continuum and line contributions separated in such a way that all coupling between continuum and line processes is included in the line contribution.

Line fluxes. - The profile across the shock layer of the line heat flux toward the body for each of the three radiation models is shown in figure 6. In the symbol key the computing time on a CDC 6600 computer is shown for each case.¹ The comparison of profiles indicates two areas of discrepancy: (1) in the air layer, where RATRAP predicts as much as 25 percent more line flux than the other models, and (2) in the ablation layer, where RADICAL predicts considerably (about 45 percent) lower flux due to more absorption of the radiation by ablation gases. While the exponential approximation could account for some of the differences between MDAC and the other two codes, it could not contribute to the significant differences between RATRAP and RADICAL. The reasons for the differences seen in figure 6 have been examined by studying the spectral detail of the flux at various points in the shock layer. The points chosen are $y/\delta = 0.76$, a point in the air layer near the shock wave; $y/\delta = 0.26$, the point at the boundary of the air and ablation layers; and $y/\delta = 0$, the point at the wall.

Figures 7(a) to (c) present the accumulative spectral integral of the line flux at the three selected points. The results for $y/\delta = 0.76$ in figure 7(a) show that for the air species the fluxes in the visible lines ($h\nu \approx 1.5$ to 3.0 eV) predicted by the MDAC code are about twice as much as those predicted by the other two codes. The MDAC code also predicts vacuum ultraviolet (VUV) line fluxes ($h\nu > 10$ eV) that are one-half to one-third of those of the other codes. The RATRAP and RADICAL spectral line fluxes are in good agreement except that RATRAP predicts about 25 percent more VUV flux than RADICAL.

¹ Calculations with a more recent version of the RATRAP code resulted in a 3.5-minute computation time instead of the 5.0-minute time with the version used herein.

Reasons for these disagreements are suggested by differences which have been noted in the model descriptions (tables I and II). For the considerable number of transitions where no line-strength data are available from references 13 and 14, the MDAC code relies on a hydrogenic model (ref. 10) and the RATRAP and RADICAL codes rely on tabulations of detailed quantum-mechanics calculations (ref. 8). Since the behavior of C, N, and O are known to be nonhydrogenic, it is believed that the latter approach is more accurate.

An additional area of differences in the models is the approach to the line-absorption-coefficient models. In the RATRAP model an "equivalent width" and "line grouping" approach is used which involves several approximations (see table II(b)). The approximation that the Planck function is constant over the line-group frequency interval has been examined by Robert E. Boughner, at Langley Research Center. Unpublished studies by Boughner have compared exact and approximate intensities of a line group in the VUV (about 12 eV) for conditions typical of those being considered. These studies showed that the approximate intensities were consistently about 10 percent higher than exact values. Therefore, the approximation of the Planck function could account for a significant portion of the difference in the VUV line flux between RATRAP and the other codes. The approximate description of the onset for line overlapping in RATRAP is the only other approximation not shared with one of the other codes. The level of error introduced by this approximation has not been established. It can be said, however, that any approximation which results in treating overlapped lines as nonoverlapping will cause an overprediction of the line transport. This effect is therefore a possible contributor to the larger VUV line flux in RATRAP compared with the other codes.

The RADICAL and MDAC codes treat lines in detail except those near the photoelectric edge, which are included by shifting the edge. RADICAL considers 11 to 15 frequency points to describe each line profile whereas MDAC considers approximately three frequency points.

Since it can be concluded from the comparison in table II that the RADICAL line model entails fewer approximations and includes more detail than the other models, the results of RADICAL are considered more realistic.

The manner in which the line flux from the air layer is attenuated as it propagates toward the body is seen by comparing figures 7(a) with 7(b) and 7(b) with 7(c). In figures 7(a) and 7(b) it is seen that the VUV line flux above 11 eV is attenuated by passing through approximately 8.5 cm of the air layer ($y/\delta = 0.76$ to $y/\delta = 0.26$), where the temperature drops from about 13 000 K to 10 000 K. Finally, from a comparison of figures 7(b) and 7(c) it is found that the infrared (IR) and visible line flux passes unattenuated to the wall, whereas all of the ultraviolet (UV) line flux is attenuated except for a region at 10.4 eV in the RATRAP calculation. To examine this discrepancy the RADICAL

code was used to make calculations with and without the H₂ molecular contributions. The results showed that without the H₂ contributions, the line flux near 10.4 eV was unattenuated as it is in RATRAP. It is therefore concluded that the appearance of VUV line flux at 10.4 eV in RATRAP and not in the other codes is a result of the window between 10 and 11 eV in the H₂ contribution in RATRAP. Without the VUV line flux at 10.4 eV there is good agreement in the line heat flux at the wall between RATRAP and RADICAL.

The spectral data shown also point out the fact that the apparent agreement between the models in figure 6 is fortuitous and that the line fluxes are in disagreement in the visible and far-UV regions.

Continuum fluxes. - The profile across the shock layer of the radiative heat flux from continuum contributions (including molecular bands) for each of the three radiation models is shown in figure 8. These results indicate that in the air layer there is a significant disagreement between the MDAC results and the other models (as much as 35 percent lower). It is noted that the deviations between MDAC and the other two codes are in the same direction as deviations caused by the exponential approximation shown in figure 5. Therefore, the continuum calculation shown in figure 8 for RATRAP was repeated with the exponential approximation deleted. Those results indicated a maximum reduction of about 5 percent near the peak of the profile as a consequence of eliminating the approximation. Thus other reasons must exist for the larger disagreement seen in figure 8. Comparisons similar to those shown for the line heat fluxes can be made to examine the source of this disagreement. At each of the three points previously used ($y/\delta = 0.76, 0.26,$ and 0), the spectral variation of the continuum flux and its accumulative integral are presented.

The results in figures 9(a) and (b) indicate that in the air layer the MDAC results disagree with the other two codes through the spectral range out to the far-UV region where the curves begin to show the effect of the blackbody function. The major areas of disagreement are in the 0 to 2 eV range, where free-free contributions dominate; in the 3 to 10 eV range, where photoionization from excited states dominates; and in the far-UV, where the main feature is the location of the predominant photoionization edge. In the RATRAP and RADICAL codes the classical hydrogenic approximation was used for the free-free contributions. In MDAC the "modified hydrogenic" model described in reference 9 was used to treat the free-free contributions. In RATRAP and RADICAL all photoionization (bound-free) contributions are based on curve fits of data (ref. 8) which were calculated by using the "quantum defect" method. In the MDAC code photoionization from excited states is treated with the modified hydrogenic model described in reference 9, and ground-state photoionization is treated with a modification of the classical hydrogenic model. (See ref. 3.) Based on the results presented herein, it is evident that these approaches are in considerable disagreement. Since the method employed in RATRAP

and RADICAL for the photoionization contributions is based on a more detailed description of the complex atom processes, it is believed to be more realistic than that used in MDAC.

The results for $y/\delta = 0.26$ in figures 10(a) and (b) show that as a result of passing through a good portion of the air layer, where temperature is decreasing, the far-UV continuum is significantly self-absorbed. The effect is that the higher near-UV flux in MDAC approximately compensates for the lower far-UV flux. This produces the deceiving result that the three programs are in fairly good agreement as far as the total spectrally integrated flux is concerned.

The results for the continuum flux which reaches the wall are shown in figure 11. From figure 11(a) it is seen that all significant continuum flux is absorbed beyond 7 or 8 eV except for a spike in the RATRAP spectrum at 10.8 eV. The importance of this spike is not readily apparent in figure 11(a) because of the logarithmic scale. Its importance is apparent in figure 11(b). The previously mentioned calculations with and without H₂ contributions have shown that this spike in the RATRAP calculation is a result of the window (10 to 11 eV) in the H₂ contributions in RATRAP. Without the spike in the RATRAP spectrum that model would predict significantly lower continuum flux at the wall compared with the other two models. The window at 6 to 7 eV in the H₂ contributions in RATRAP was found to change the shape of the cutoff of the spectral flux in the 6 to 8 eV range but to have very little influence on the integrated flux.

Figure 11(b) indicates that if the spike in the RATRAP spectrum at 10.8 eV did not exist, a significant difference would exist between the wall continuum heat fluxes of RATRAP and RADICAL. This is a surprising observation because the methods of treating the continuum in the two codes are very nearly the same (see table II(a)). The only exception to the approaches is the modification to the low-frequency continuum from Biberman and Norman (ref. 7) which is made in RADICAL but not in RATRAP. Calculations without this modification in RADICAL have shown that it accounts for the major portion (about 70 percent) of the difference which would exist. The remainder of the difference was found to be due to the inclusion of photodetachment effects (O⁻ and N⁻ shown in table III) and merged IR lines as part of the continuum in RADICAL but not in RATRAP. The merged IR lines are those referred to in table II(b) as involving transitions with lower levels having large principal quantum numbers.

CONCLUDING REMARKS

A comparison of the radiation flux profiles and spectral distributions from three detailed nongray radiation models has been made for shock-layer conditions representative of manned earth reentry from an interplanetary mission. The results have shown

that significant differences exist in the radiation flux computed by the three models. For the comparisons the calculations were divided into line and continuum contributions.

The comparison of line fluxes has shown that in the air layer the differences in the models are significant in the visible and far-ultraviolet (UV) regions of the spectra. Because the line model in RADICAL involves fewer approximations and includes more detail, it is believed to be more realistic than the other models. Results for the attenuation of the line flux by the boundary layer have shown that whereas the infrared and visible flux is unattenuated, the UV flux is completely absorbed except at 10.4 eV in RATRAP. This unattenuated flux was determined to be a result of a window between 10 and 11 eV in the H₂ contribution in RATRAP.

The comparison of continuum fluxes has shown that the MDAC results are in considerable disagreement with those from the other two codes. Since the method of treating the photoionization continuum in RATRAP and RADICAL is based on a more realistic nonhydrogenic model, it is considered to be more accurate than the hydrogenic model used in MDAC. Results for the attenuation of the continuum flux by the boundary layer have shown that all UV flux beyond 7 to 8 eV is absorbed except for a spike in the RATRAP results at 10.8 eV. This spike was found to be due to the window in the H₂ contribution in RATRAP which was also noted in the line flux results.

In general the RADICAL model was found to depend on fewer approximations, to include more detail, and to require less computer time than the other two models.

Langley Research Center,
National Aeronautics and Space Administration,
Hampton, Va., December 9, 1971.

REFERENCES

1. Smith, G. Louis; Suttles, John T.; Sullivan, Edward M.; and Graves, Randolph A., Jr.: Viscous Radiating Flow Field on an Ablating Blunt Body. AIAA Paper No. 70-218, Jan. 1970.
2. Wilson, K. H.: Massive Blowing Effects on Viscous, Radiating, Stagnation-Point Flow. AIAA Paper No. 70-203, Jan. 1970.
3. Rigdon, W. S.; Dirling, R. B., Jr.; and Thomas, M.: Stagnation Point Heat Transfer During Hypervelocity Atmospheric Entry. NASA CR-1462, 1970.
4. Wilson, K. H.: RATRAP - A Radiation Transport Code. 6-77-67-12, Lockheed Missiles & Space Co., Mar. 14, 1967.
5. Nicolet, William E.: Advanced Methods for Calculating Radiation Transport in Ablation-Product Contaminated Boundary Layers. NASA CR-1656, 1970.
6. Wilson, K. H.; and Greif, R.: Radiation Transport in Atomic Plasmas. J. Quant. Spectry. Radiat. Transfer, vol. 8, no. 4, Apr. 1968, pp. 1061-1086.
7. Biberman, L. M.; and Norman, G. E.: Rekombinatsionnoye i Tormoznoye Izlucheniye Plazmy (Emission of Recombination Radiation and Bremsstrahlung From Plasma). J. Quant. Spectry. Radiat. Transfer, vol. 3, no. 3, July-Sept. 1963, pp. 221-245.
8. Wilson, K. H.; and Nicolet, W. E.: Spectral Absorption Coefficients of Carbon, Nitrogen and Oxygen Atoms. J. Quant. Spectry. Radiat. Transfer, vol. 7, no. 6, Nov.-Dec. 1967, pp. 891-941.
9. Penner, S. S.; and Thomas, M.: Approximate Theoretical Calculations of Continuum Opacities. AIAA J., vol. 2, no. 9, Sept. 1964, pp. 1572-1575.
10. Thomas, M.: The Spectral Linear Absorption Coefficients of Gases - Computer Program SPECS (H189). DAC-59135, Missile Space Syst. Div., Douglas Aircraft Co., Inc., Dec. 1966. (Revised, May 1967.)
11. Hoshizaki, H.; and Lasher, L. E.: Convective and Radiative Heat Transfer to an Ablating Body. 4-06-66-12 (Contract NAS 7-386), Lockheed Missiles & Space Co., July 1966. (Available as NASA CR-73060.)
12. Patch, R. W.; Shackelford, W. L.; and Penner, S. S.: Approximate Spectral Absorption Coefficient Calculations for Electronic Band Systems Belonging to Diatomic Molecules. J. Quant. Spectry. Radiat. Transfer, vol. 2, July/Sept. 1962. pp. 263-271.

13. Griem, Hans R.: Plasma Spectroscopy. McGraw-Hill Book Co., c.1964.
14. Wiese, W. L.; Smith, M. W.; and Glennon, B. M.: Atomic Transition Probabilities.
Vol. I - Hydrogen Through Neon. NSRDS-NBS 4, U.S. Dep. Com., May 20, 1966.

TABLE I.- FEATURES OF METHODS USED IN TRANSPORT CALCULATIONS

<p>RATRAP (refs. 4 and 6)</p>	<p>RADICAL (ref. 5)</p>	<p>MDAC (ref. 3)</p>
<p>Local thermodynamic equilibrium Plane slab Transfer equation reduced analytically to a quadrature expression for heat flux Exponential approximation Linear spatial integration in terms of emissivity Linear-frequency integration</p>	<p>Local thermodynamic equilibrium Plane slab Transfer equation reduced analytically to a quadrature expression for heat flux Exponential approximation Cubic spatial integration in terms of emissivity Linear-frequency integration</p>	<p>Local thermodynamic equilibrium Plane slab Numerical integration of trans- fer equation for intensity Gaussian quadrature (eight-point) for solid angle integration Second-order Runge-Kutta spatial integration Linear-frequency integration</p>

TABLE II. - ABSORPTION-COEFFICIENT MODELS

(a) Continuum (includes molecular bands)

	RATRAP (refs. 6, 11)	RADICAL (ref. 5)	MDAC (ref. 3)
Continuum	Low frequency	Free-free and bound-free using Biberman and Norman (ref. 7)	Free-free and bound-free from modified hydrogenic model (ref. 9)
	High frequency	Free-free from classical hydrogenic model Bound-free from Wilson and Nicolet (ref. 8)	Free-free modified hydrogenic model (ref. 9) Bound-free modified hydrogenic model (refs. 3, 10)
Molecular bands (treated as a pseudo-continuum)	"Smeared line" model (refs. 11, 12)	"Smeared line" model and "bandless" model (refs. 12, 5)	"Smeared line" model (refs. 3, 12)

TABLE II. - ABSORPTION-COEFFICIENT MODELS - Concluded

(b) Atomic lines

RATRAP (ref. 6)	RADICAL (ref. 5)	MDAC (ref. 3)
<p>"Equivalent width" and "line grouping" formulation wherein: Restricted to Lorentz shape and electron-impact broadening Planck function and continuum absorption coefficient constant over line-group frequency interval Spatial integration in terms of group equivalent width Isolated lines integrated closed form over frequency for group equivalent width Overlapping when group average equivalent width is of order of average line spacing for group Overlapped lines integrated numerically over frequency for group equivalent width Line strengths and half-widths from Wilson and Nicolet (ref. 8) Lines near photoionization edge treated by edge shift</p>	<p>All lines treated individually except: Lines near photoionization edge treated by edge shift Transitions with lower levels having large principal quantum number treated as a continuum Lines grouped only to determine which lines may overlap Line shapes and half-widths by Lorentz shape with half-width from electron-impact and resonance effects Shape and half-width from Doppler effects Line strengths and electron-impact half-widths from Wilson and Nicolet (ref. 8) 11 to 15 frequency points used for each line</p>	<p>All lines treated individually except those near photoionization edge which are treated by edge shift All lines have Lorentz shape with half-widths from electron-impact theory (ref. 10) Line strengths from Griem (ref. 13) and NBS (ref. 14) where possible and from hydrogenic model elsewhere Three frequency points used to describe each line</p>

TABLE III. - RADIATION CONTRIBUTIONS FROM ATOMIC (AND IONIC) SPECIES

Species	RATRAP (Lockheed)		RADICAL (Aerotherm)		MDAC (McDonnell Douglas)	
	Lines	Continuum	Lines	Continuum	Lines	Continuum
N	X	X	X	X	X	X
O	X	X	X	X	X	X
C	---	X	X	X	X	X
H	---	X	X	X	X	X
N ⁺	X	X	X	---	X	X
O ⁺	X	X	X	---	X	X
C ⁺	---	X	X	---	X	X
O ⁻ , C ⁻ , H ⁻	---	---	---	X (N ⁻ also)	---	X

TABLE IV.- RADIATION CONTRIBUTIONS FROM MOLECULAR SPECIES

Species	RATRAP (Lockheed)		RADICAL (Aerotherm)		MDAC (McDonnell Douglas)	
	No. bands included	Spectral range, eV	No. bands included	Spectral range, eV	No. bands included	Spectral range, eV
C ₂	4	1.8 to 6	3	1.8 to 6	5	0 to 8.5
H ₂	1	11 to 15.5	2	3.6 to 15.5	2	7.5 to 15
CO	1	7 to 10	1	4.3 to 10.6	5	0 to 11
N ₂	1	11 to 14.4	3	0.75 to 4.5 6.5 to 12.8	5	0.5 to 5 9 to 13
O ₂	1	7 to 9.2	2	3 to 9.2	1	6.5 to 10
NO	---	-----	4	2.7 to 13.5	4	2.5 to 8.5
C ₂ H ₂	---	-----	---	-----	1	6 to 11.5
CH	---	-----	---	-----	2	2.5 to 4.5
C ₃	---	-----	---	-----	1	2.5 to 3.5
CN	1	2 to 6	2	0.8 to 6	3	0 to 7.5
N ₂ ⁺	---	-----	1	2.2 to 4.5	1	2.1 to 4.2

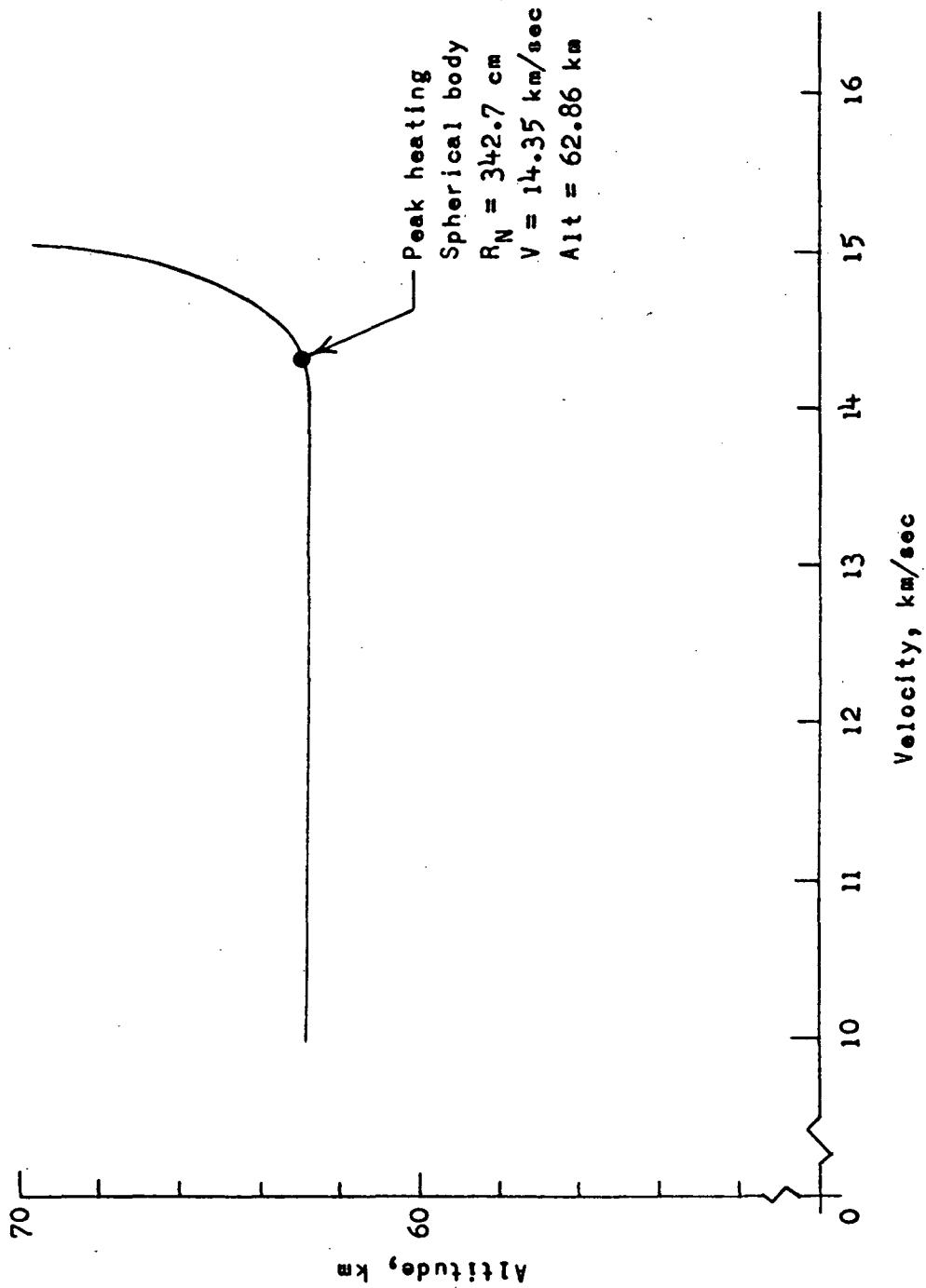


Figure 1.- Typical lifting entry used for the study. $V_E = 15.24$ km/sec; $\gamma_E = 6.33^\circ$; $L/D = 0.5$; and $W/C_{DA} = 3950$ N/m².

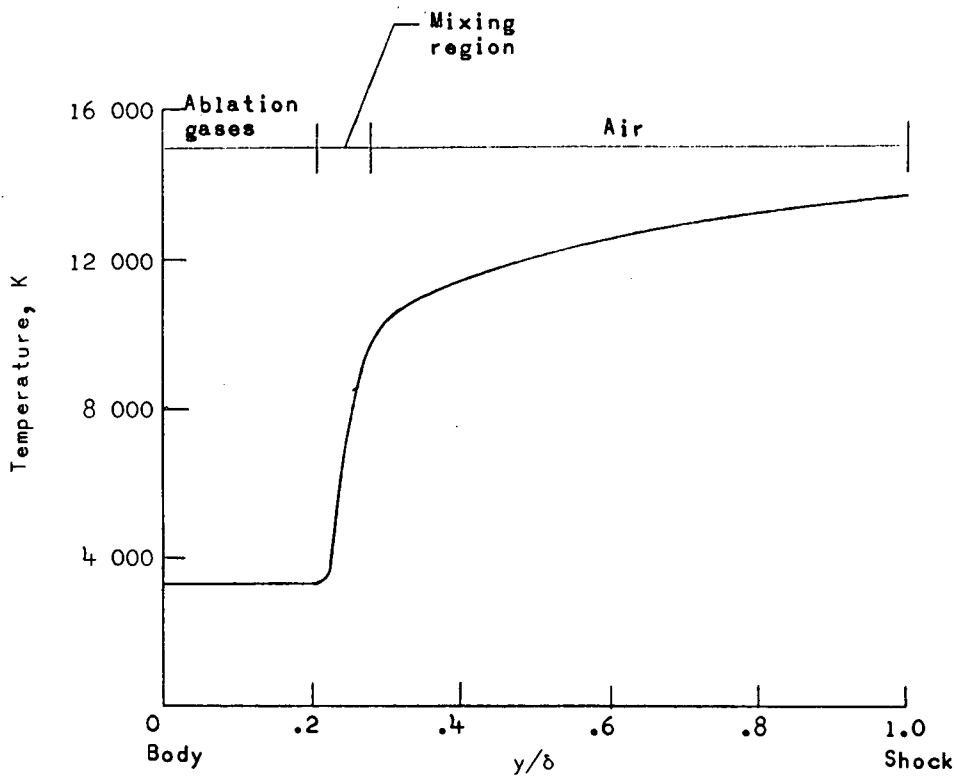


Figure 2.- Stagnation-line temperature profile used in the study.

$p_{\text{shock}} = 0.41 \text{ atm}; \delta = 16.94 \text{ cm}.$

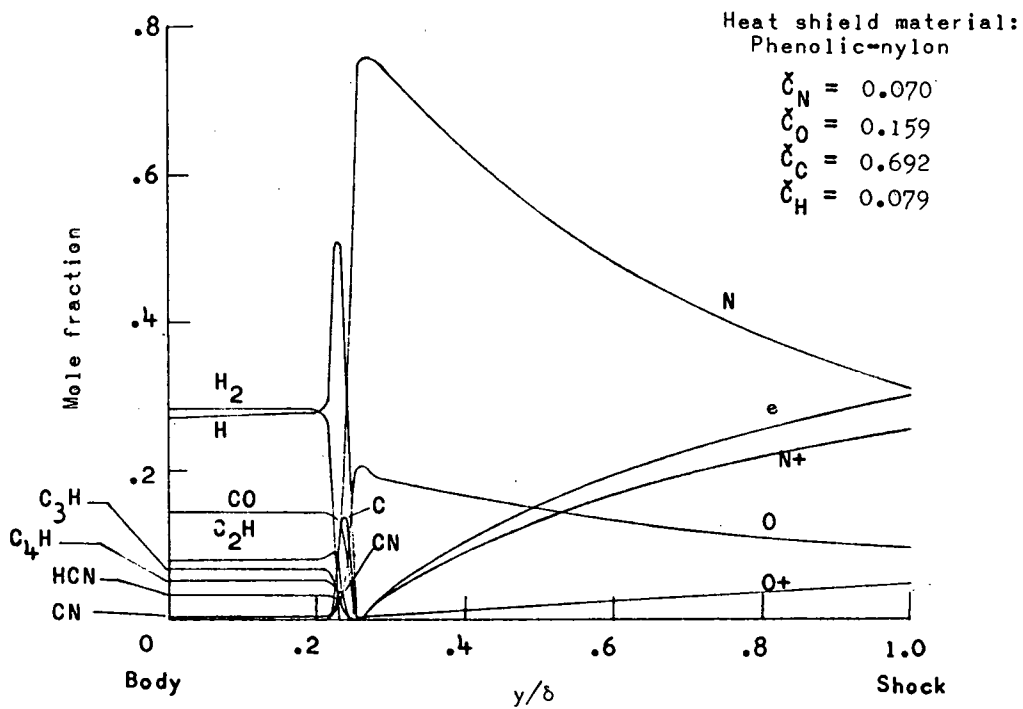


Figure 3.- Stagnation-line species mole-fraction profiles used in the study.

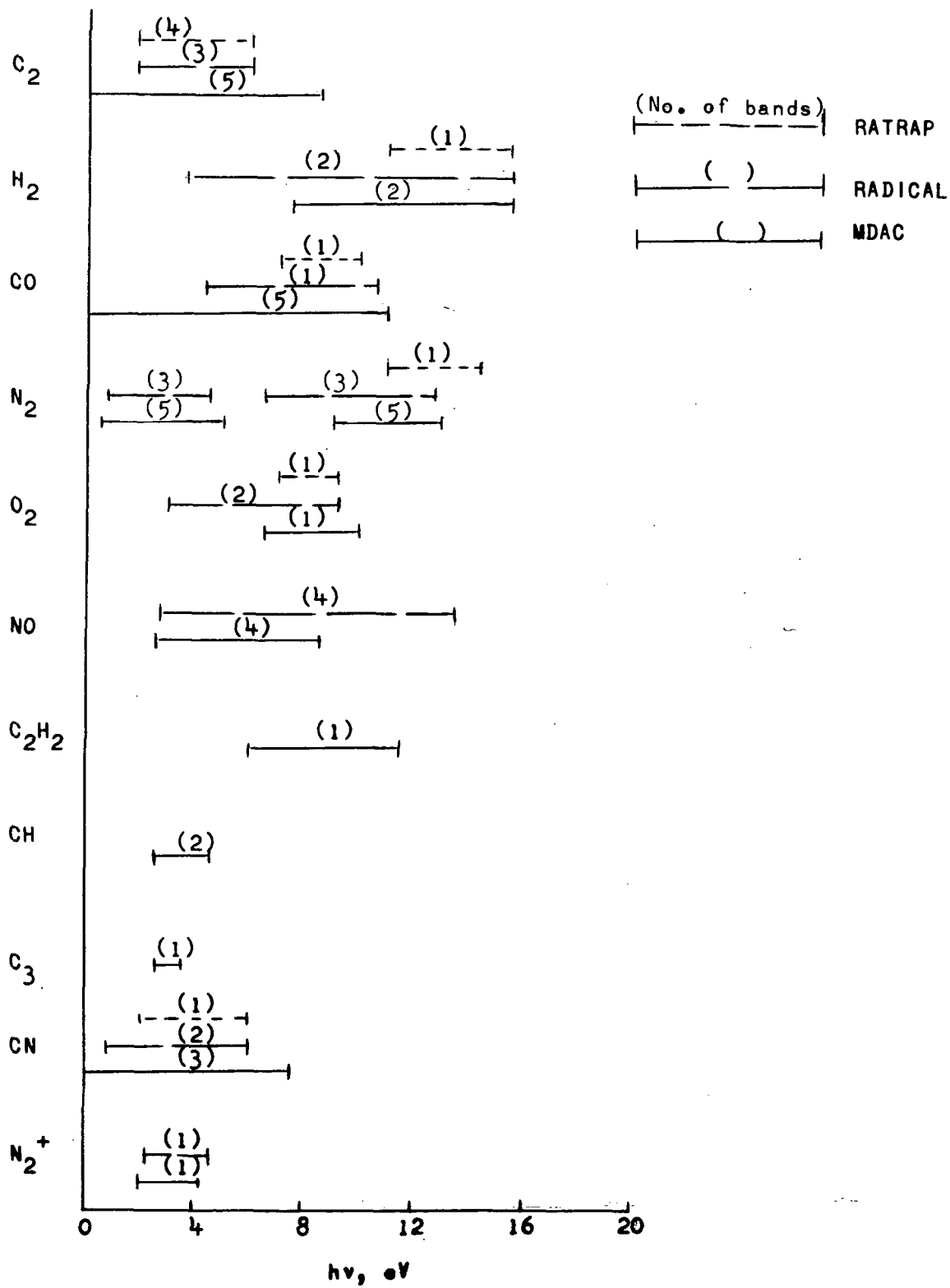


Figure 4.- Graphical representation of radiation contributions from molecular species.

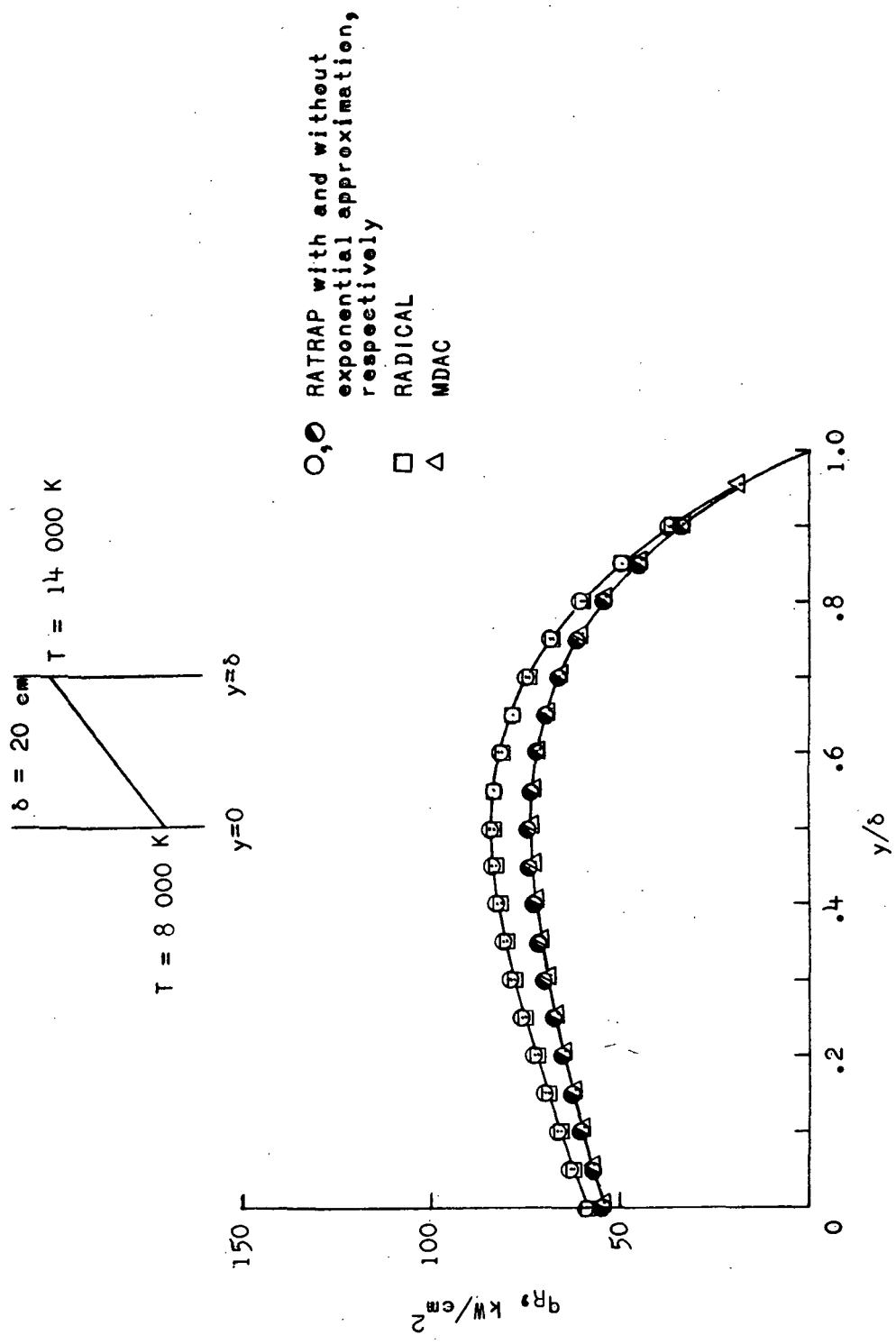


Figure 5.- Comparison of heat fluxes toward body ($y = 0$) for a gas with a gray absorption coefficient (0.05 cm^{-1}) and a linear temperature distribution.

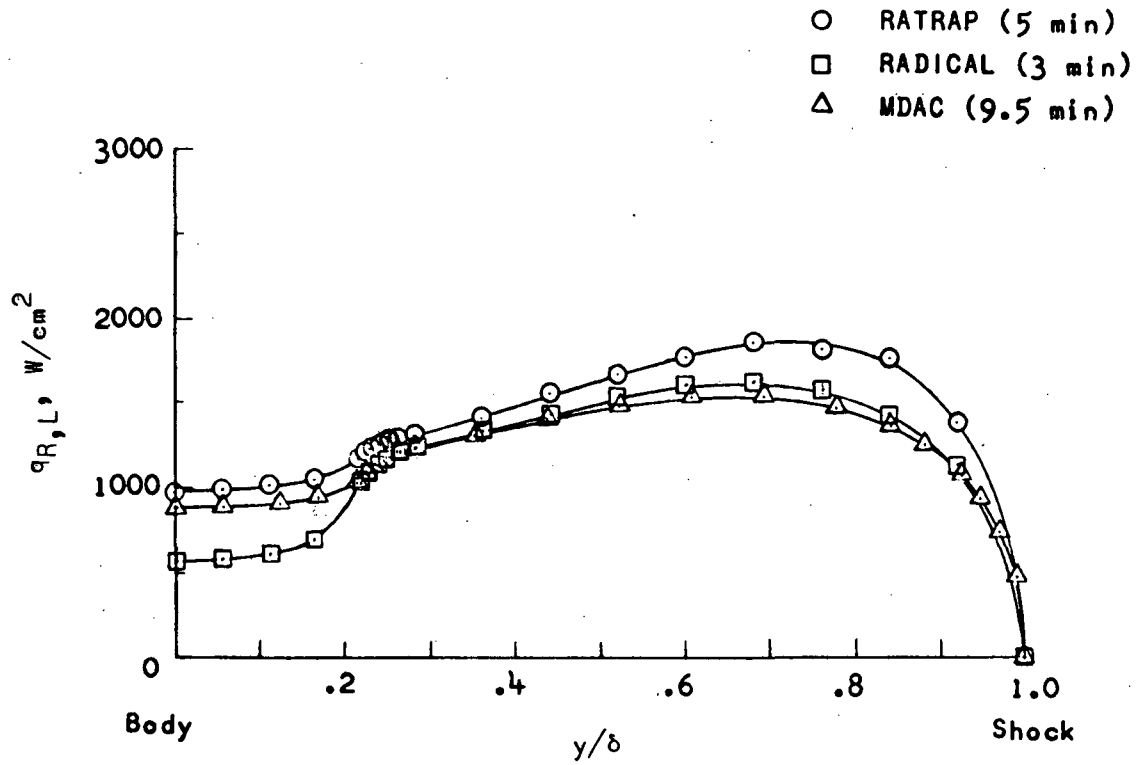
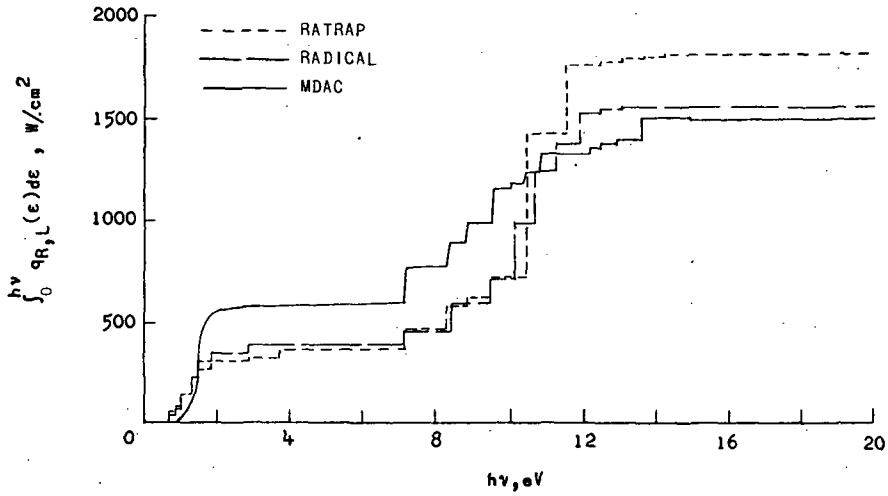
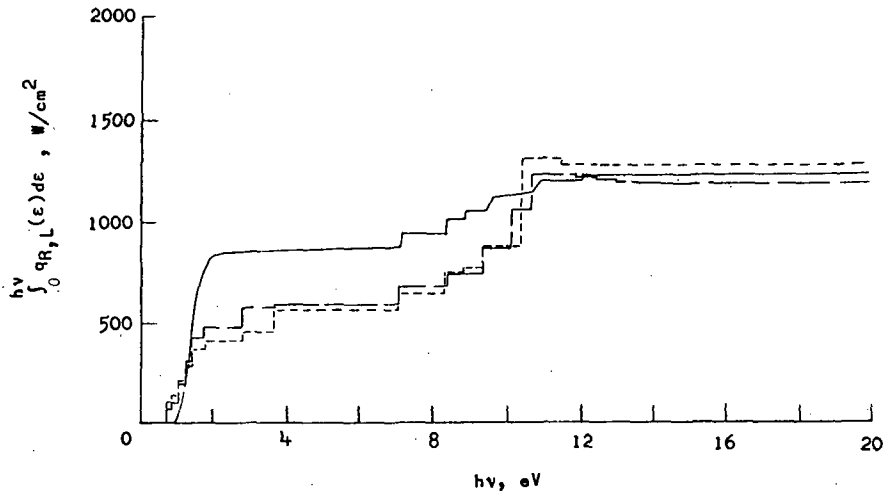


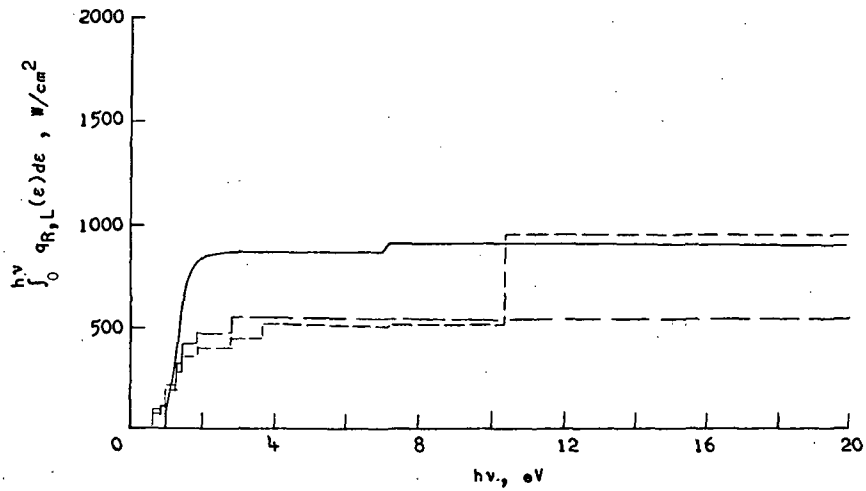
Figure 6.- Profile of line heat flux toward body. (Calculation times are shown in symbol key in parentheses.)



(a) $y/\delta = 0.76$.



(b) $y/\delta = 0.26$.



(c) $y/\delta = 0$.

Figure 7.- Accumulative spectral integral of line flux.

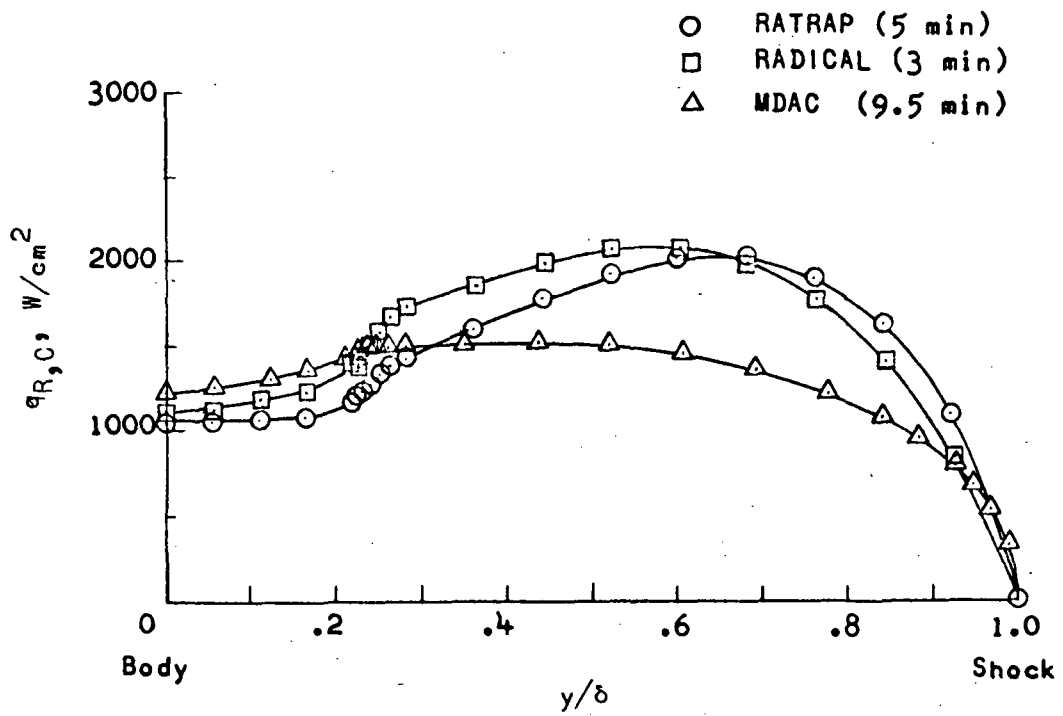
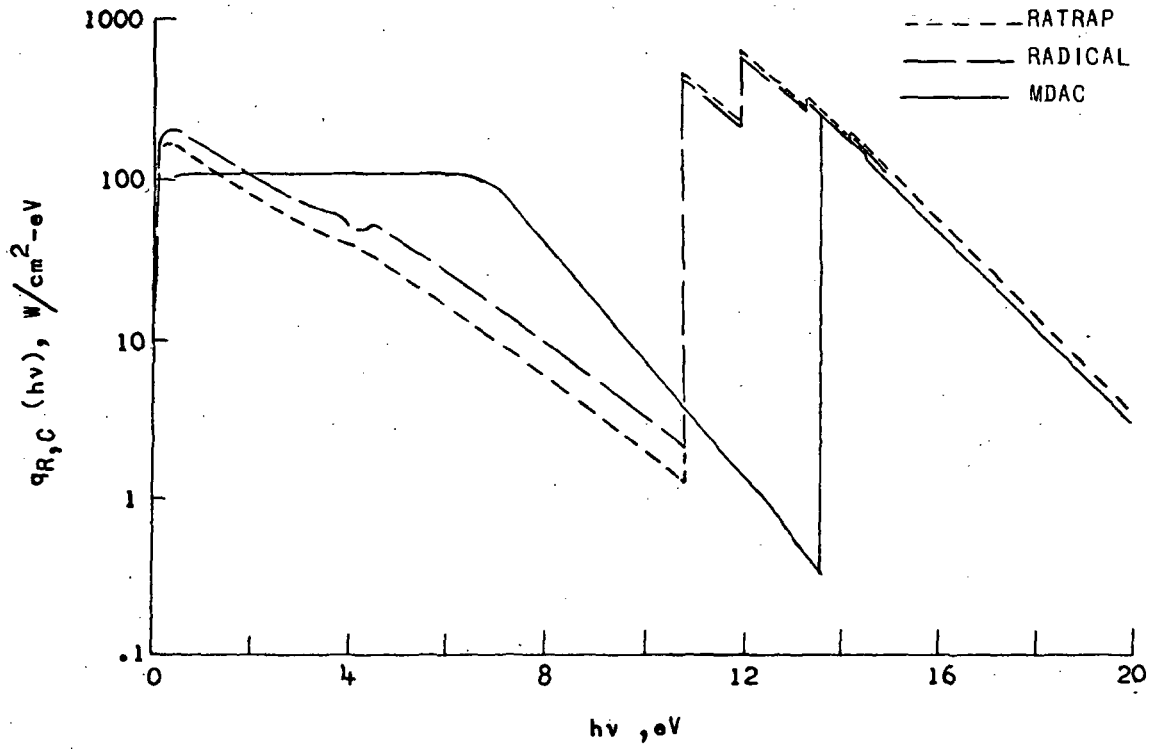
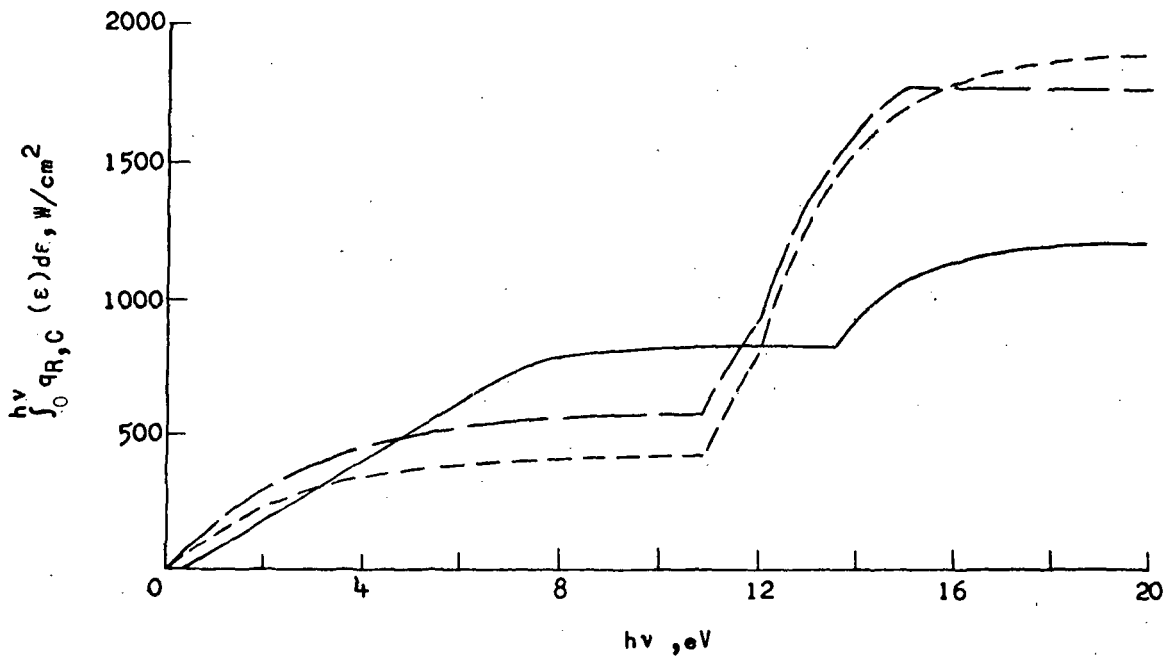


Figure 8.- Profile of continuum heat flux toward body. (Calculation times are shown in symbol key in parentheses.)

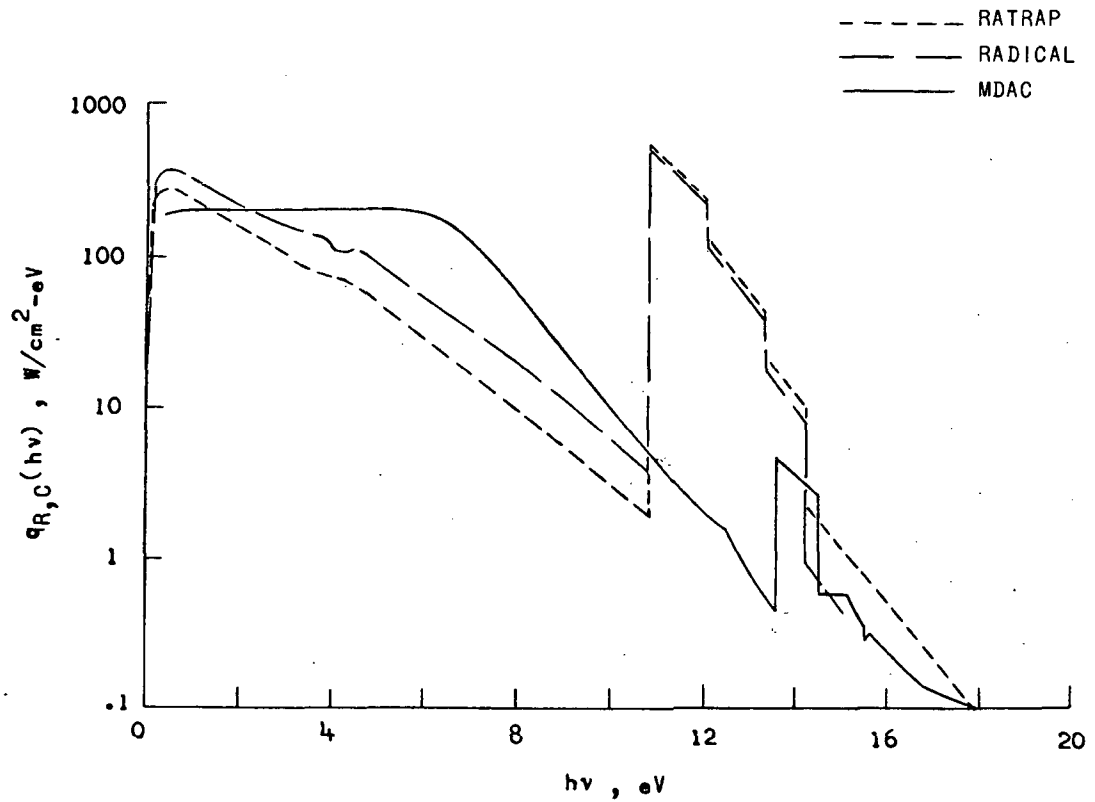


(a) Spectral.

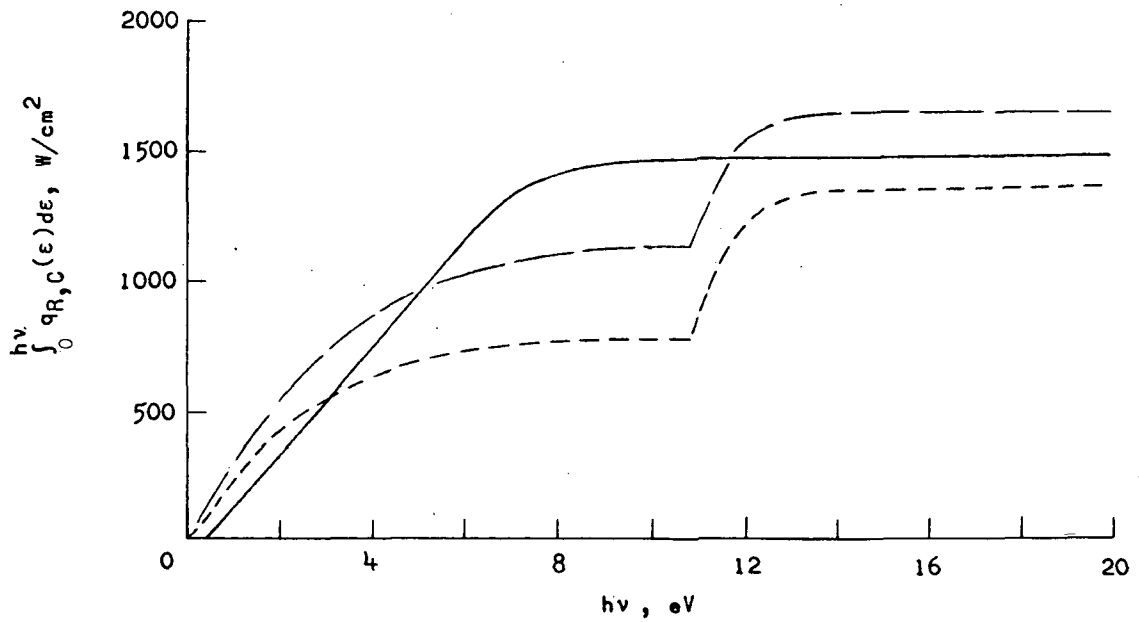


(b) Accumulative spectral integral.

Figure 9.- Continuum heat flux at $y/\delta = 0.76$.

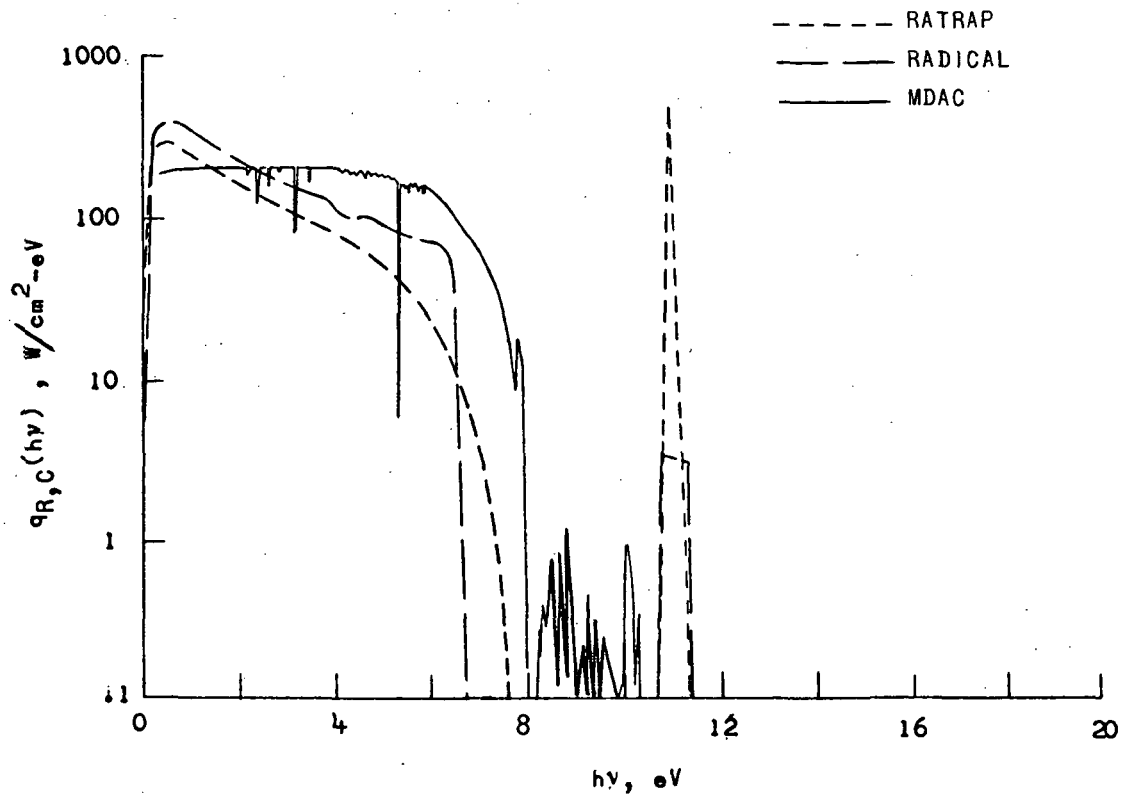


(a) Spectral.

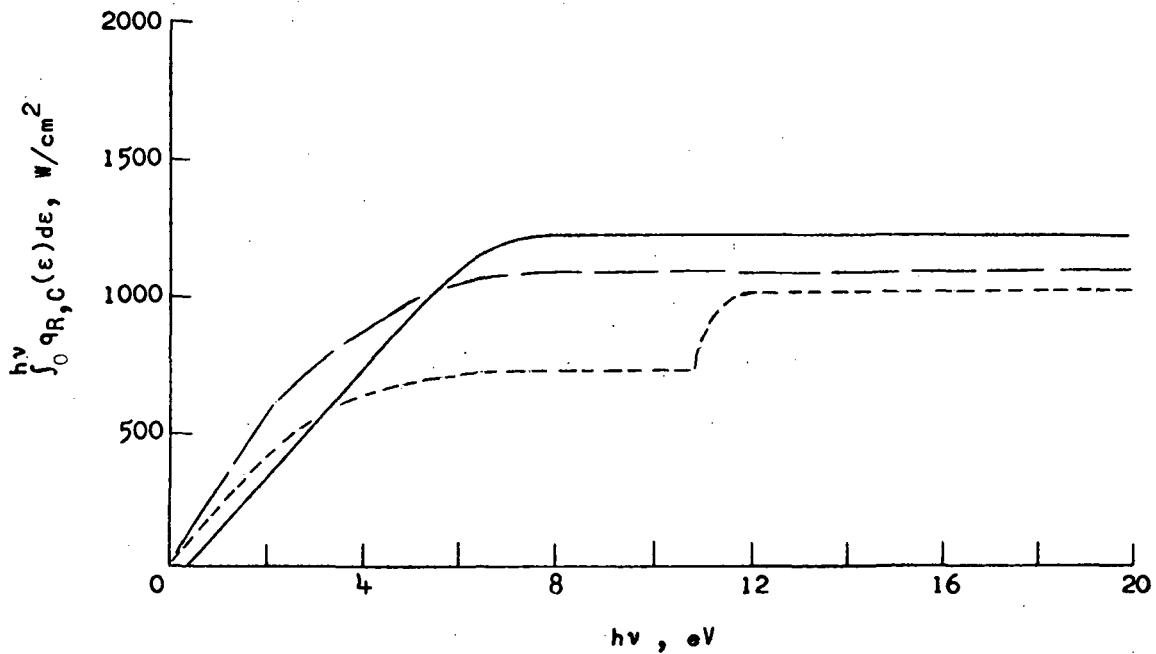


(b) Accumulative spectral integral.

Figure 10.- Continuum heat flux at $y/\delta = 0.26$.



(a) Spectral.



(b) Accumulative spectral integral.

Figure 11.- Continuum heat flux at $y/\delta = 0$.



POSTMASTER: If Undeliverable (Section 158
Postal Manual) Do Not Return

"The aeronautical and space activities of the United States shall be conducted so as to contribute . . . to the expansion of human knowledge of phenomena in the atmosphere and space. The Administration shall provide for the widest practicable and appropriate dissemination of information concerning its activities and the results thereof."

— NATIONAL AERONAUTICS AND SPACE ACT OF 1958

NASA SCIENTIFIC AND TECHNICAL PUBLICATIONS

TECHNICAL REPORTS: Scientific and technical information considered important, complete, and a lasting contribution to existing knowledge.

TECHNICAL NOTES: Information less broad in scope but nevertheless of importance as a contribution to existing knowledge.

TECHNICAL MEMORANDUMS: Information receiving limited distribution because of preliminary data, security classification, or other reasons.

CONTRACTOR REPORTS: Scientific and technical information generated under a NASA contract or grant and considered an important contribution to existing knowledge.

TECHNICAL TRANSLATIONS: Information published in a foreign language considered to merit NASA distribution in English.

SPECIAL PUBLICATIONS: Information derived from or of value to NASA activities. Publications include conference proceedings, monographs, data compilations, handbooks, sourcebooks, and special bibliographies.

TECHNOLOGY UTILIZATION PUBLICATIONS: Information on technology used by NASA that may be of particular interest in commercial and other non-aerospace applications. Publications include Tech Briefs, Technology Utilization Reports and Technology Surveys.

Details on the availability of these publications may be obtained from:

SCIENTIFIC AND TECHNICAL INFORMATION OFFICE

NATIONAL AERONAUTICS AND SPACE ADMINISTRATION

Washington, D.C. 20546